Check for updates

J Surfact Deterg (2021) **24:** 783–800
DOI 10.1002/jsde.12494

ORIGINAL ARTICLE

# Structural Investigation of Diol and Triol Poly(oxypropylene)-Poly(oxyethylene) Block Copolymers Micelles: Composition Dependence, Temperature Response and Clouding Behavior

**Cilâine Verônica Teixeira[1] · Yuri Alencar Marques[2] · Márcia Carvalho de Abreu Fantini[3] · Diomar da Rocha Santos Bittencourt[3] · Cristiano Luís Pinto Oliveira[3]**

Received: 3 November 2020 / Revised: 12 January 2021 / Accepted: 5 February 2021
© 2021 AOCS.

**Abstract** Solution behavior of two commercially used polyether glycols with poly(oxyethylene) (PEO)-poly (oxypropylene) (PPO)-poly(oxyethylene) (PEO) triblock composition—Diol (linear) and Triol (star-like)—was studied, concerning the concentration and temperature effects until the cloud point (CP). 2-(2-butoxyetoxy) ethanol (DB) increased their miscibility with water. The structural study was performed with 25% DB in water, which produced isotropic solutions at room temperature at all polymer concentrations. Micelle's formation was only observed above 40% of polymer, when reversed micelles were formed. The solvent nuclei of the reversed micelles increased with increasing polymer concentrations, caused by dehydration of the PPO chains, then decreased at further higher concentrations, with completely dehydrated hydrophobic chains. When CP is reached, the solvent nuclei are separated by large polymer domains, without phase separation. Neither ordered nor gel phase was formed, probably due to a combination of high miscibility and short hydrophobic segments. The study was performed by Small-Angle X-ray scattering (SAXS) and complemented by Fourier-transformed infrared spectroscopy (FTIR) and dynamic light scattering (DLS). The main contribution of this work is based on the fact that the knowledge of the solubility behavior of Diol and Triol, by changing the solvent or temperature, opens up new possibilities of their use to phase separation processes in industrial applications and delivery systems. Moreover, the elucidation of mechanisms of solubility allows for the design of novel polyether glycols with tailored solution behavior for efficient performance in its target use. All applications rely on their solution behavior and can be benefited from the present results.

**Keywords** Cloud point · Triblock · Copolymer · Glycol · SAXS · Small-angle scattering

*J Surfact Deterg* (2021) **24:** 783–800.

**Supporting information** Additional supporting information may be found online in the Supporting Information section at the end of the article.

✉ Cilâine Verônica Teixeira
cilaineteix@if.ufrgs.br

[1] Physics Institute, Federal University of Rio Grande do Sul, Brazil

[2] Dow, Polyurethanes Research and Development, Freeport, Texas, USA

[3] Physics Institute, University of São Paulo, Brazil

## Introduction

Polyether glycol polymers, formed by the combination of different polymeric chains, can change their physicochemical, interfacial properties, and solution behavior when dissolved in aqueous solution (Alexandridis and Hatton, 1995; Booth and Attwood, 2000; Ivanova et al., 2000), presenting amphiphilic character and self-assembly properties. Special attention has been devoted to triblock copolymers, which aggregate in solution in the form of micelles (Brown et al., 1991; Malmsten and Lindman, 1992; Mortensen and Pedersen, 1993; Reddy et al., 1990; Wanka et al., 1990; Zhou and Chu, 1988b). In particular, triblock copolymers with PEO-PPO-PEO structure, where PEO is polyethylene oxide and PPO is polypropylene oxide, form a big copolymer family, normally called polaxamers, obtained by variation of chain lengths and PEO:PPO ratio. The micelles

Published online: 31 March 2021
J Surfact Deterg (2021) **24:** 783–800

formed in aqueous solution have a core predominantly formed by PPO and a corona formed by hydrated PEO blocks (Mortensen, 1992). Different chain lengths and PEO:PPO ratio are responsible for different polymer hydrophobicity/hydrophilicity (Holmberg et al., 2002), causing a rich polymorphism of structures formed in water and other solvents (Alexandridis, 1997; Liu et al., 1997b). The polymer concentration and solvent conditions strongly influence the micelles shape, size, and phase, as well as the possibility of formation of ordered and liquid-crystal phases (Alexandridis et al., 1998; Alexandridis and Hatton, 1995; Chaibundit et al., 2007; Israelachvili et al., 1976; Lobry et al., 1999). The presence of a co-solvent (Desai et al., 2001; Ivanova et al., 2000; Pandit and Mclntyre, 1997), salt (Alexandridis and Holzwarth, 1997; Teixeira et al., 2011), and temperature variation (Wanka et al., 1994) have a strong effect on the chains' hydration and consequently on the micelles' shape or phase. Reverse micelles have also been observed for some copolymer structures, concentrations, and solvent conditions (Alexandridis et al., 1996; Alexandridis and Andersson, 1997; Chu, 1995).

Several block copolymers, and especially those containing relatively high molecular weight PEO blocks (Dormidontova, 2004; Kwon and Okano, 1996; Lee et al., 1995) are biocompatible, and this makes the structures formed in solution promising for pharmaceutical use, for surface modification, drug delivery (Allen et al., 1999; Davaran et al., 2017; Kwon and Okano, 1996; Lee et al., 1995; Miyazaki et al., 1992, 1995; Sharma et al., 2008b), and other related applications (see (Alexandridis and Hatton, 1995) and references therein) Poloxamers are also good carriers of DNA for gene therapy (Pitard et al., 2002).

The structure used for drug delivery depends on the carried species and on the different administration, that might be, for example, parenteral (micelles), oral (micellar clusters), or subdermal and topical administration (gel depots) (Cambon et al., 2014). The performance of drug solubility and delivery by micelles depends directly on the micelle sizes, size of hydrophobic cores, and the compatibility of hydrophobic drugs with the hydrophobic segments. When gel is used, the system should form a gel at physiological temperatures (Sharma et al., 2008a).

The behavior of the polyether glycols in selective solvent, primarily in polar aqueous solutions, has been an important subject in fundamental and applied research (Cambon et al., 2014; Etampawala et al., 2016; Liu et al., 1997a; Parekh et al., 2012; Wang and Feng, 2010). Yet, one of the most remarkable characteristics of polyether glycols is their lower critical solution temperature (LCST) behavior in polar selective solvents, commonly referred to as cloud point (CP). The CP of a system containing a polymer is identified as the temperature at which the polymer becomes extremely hydrophobic and a micro-phase separation occurs, causing a sharp decrease in transmittance of visible light, hence being known as "clouding." This point, and the formation of a two-phase system, can be applied for compounds extraction (Hinze and Pramauro, 1993; Watanabe and Tanaka, 1978).

The phase behavior of polyether glycols in aqueous systems, in particular the critical "clouding" behavior characterized by the CP is critical to the industrial use of these polymers in applications such as synthetic metalworking fluids and foam control especially in biological fermentation processes. The use of polyether glycols in water-based metalworking fluids relies on the LCST behavior and the ability to form concentrated polymer films on the hot metal surface that contact the fluid during cutting, drilling, quenching, and other metal-working processes (Brown, 1994). The microphase separation of the polymer-rich phase enables a lubricant layer for the metal-to-metal contact as the localized surface temperatures rise during the process, while the aqueous phase provides cooling. Skold and co-workers (Misra and Skold, 2001); (Bajouk and Skold, 2003; Misra and Skold, 2000) have indicated that the mechanisms of phase behavior of polyether glycols could impact significantly the performance of water-based metalworking fluids and the proper design of the polymer could make the polyether glycols even more effective in this application.

Studies by Németh, Scamehorn, and their co-workers (Chaisalee et al., 2003; Németh et al., 1998) have observed a reasonably disseminated description of the foam control effect of polyether amphiphilic molecules in aqueous systems, where the coacervates or close packed micelles formed by the polymers at the micro-phase separation that occurs at the CP generates a hydrophobic droplet like species that destabilizes the interfacial forces by forming discontinuous insoluble domains and thus breaking the foam lamellae and causing foam destabilization. The same mechanism of a hydrophobic droplet formed by the poliether glycol at CP in the lamellae of the foam has been reviewed by Pelton (Pelton, 2002), where it is suggested as an effective foam control in fermentation processes, which are quite challenging foaming systems due to the combination of high airflow and the abundance of foam stabilizing components in broths such as proteins and other cellular structures or metabolites. Therefore, the more detailed aspects of the behavior of polyether glycols during CP are fundamental to the elucidation and improvement of industrial foam control processes where multi-million pounds of polyether glycols are used globally.

The CP has been largely studied on linear triblock copolymers (Liu et al., 1997a; Patel et al., 2010a, b; Wang and Feng, 2010). Few studies include the effect of the functionality (number of terminal hydroxyl groups) in the hydration of PEO groups (Akinshina et al., 2015; Dormidontova,

2004; Kadam et al., 2010). According to Dormidontova (Dormidontova, 2004), the PEO segments and their terminal groups interact *via* hydrogen-bonding among themselves and with the solvent, and the water molecules also interact with each other *via* hydrogen-bonding. The competition between these interactions (PEO–PEO, PEO–water, and water–water) is responsible for the decrease of miscibility and consequent clouding when the temperature increases.

The effect of short and long chain alcohols in the miscibility of PEO and PPO segments and the consequent formation of copolymer's micelles has also been studied and related to hydrogen-bonding (Parekh et al., 2012).

Particularly for amphiphilic poly(alkylene oxide), such as PPO-PEO block copolymers, the CP in water and aqueous nonionic polar systems has been used as the main characterization parameter of commercial industrial products (Schönfeldt, 1969). It has been demonstrated that commercially produced poly(alkylene oxides) of the ABA and BAB types have a clouding behavior in water, which takes place in a temperature range that can be of several degrees until a significant cloudiness, measured by light transmittance, is detected (Zhou and Chu, 1988a, 1994). Prior to clouding, the changes in hydration of the different polymer segments can cause modifications in the micelles structure and in the system phase (isotropic, gel liquid-crystalline) (Wanka et al., 1994). The effect of temperature on the structural behavior of triblock copolymers has been extensively studied (Davaran et al., 2017; Foster et al., 2009; Herfurth et al., 2016; Mortensen and Pedersen, 1993; Pillai et al., 2016). All the cited works observed an increase of aggregates or micelles size when temperature increased, for pure (Davaran et al., 2017; Foster et al., 2009; Herfurth et al., 2016; Mortensen and Pedersen, 1993; Pillai et al., 2016) and with solubilized drugs (Foster et al., 2009), for linear (Foster et al., 2009; Mortensen and Pedersen, 1993) and star-like (Davaran et al., 2017; Herfurth et al., 2016; Pillai et al., 2016) block copolymers, when direct micelles were formed.

Some polymers with interesting structure for commercial applications have poor miscibility with water. To increase their miscibility, a solution of water and 2-(2-butoxyethoxy) ethanol is normally used, which has been largely employed in the characterization of alkylene oxide adducts in the manufacturing of commercial products. This solvent also narrows the clouding temperature range, facilitating a more accurate and sharp detection of decrease in light transmittance (Schönfeldt, 1969).

Given the fundamental importance of the temperature in the systems that present LCST, either in the aqueous behavior of PPO-PEO copolymers or in its industrial characterization, it is extremely important to understand and correlate the molecular structure of the polymers with the structures formed in solution. Details of the dependence as a function of the system concentration, temperature, and the possible differences in the CP of different structures are certainly important parameters.

In this work, we investigate two commercially available PPO-PEO block copolymers produced by Dow Chemical, with different structures, but having similar PEO:PPO ratio: Diol (with linear structure) and Triol (with a star-like structure with three PEO chains).

The aim of this study was to evaluate their behavior in solution and self-assembly structural phenomena. These two industrial amphiphilic polyether glycol block copolymers have different chemical structures and close CP temperature. The LCST curves of both copolymers in water and in a solvent solution of water and 2-(2-butoxyethoxy) ethanol (ether butyl diglycol) are presented for a large range of concentrations. The structural behavior of both polymers is obtained by Small-angle X-ray scattering (SAXS), Attenuated total reflectance Fourier-transformed infrared spectroscopy (ATR-FTIR) and dynamic light scattering (DLS) investigations.

## Experimental Section

### Materials

Two polyether glycols, industrially produced by Dow, Diol and Triol (Fig. 1a, b) were used as-synthesized in all experiments. Distilled water and 2-(2-butoxyetoxy) ethanol (DB) by Dow Chemical were used for the preparation of solvent. The solvent used was prepared with 75% distilled water and 25% DB and referred to as 25 dB.

### Methods

#### *Cloud Point Determination*

A Mettler FP900 Thermal System equipped with FP81 C photocell was used, with light of 24 V–2 W. Samples were heated at a rate of 5 °C/min, at atmospheric pressure. The CP was obtained when the visible light transmitted by the sample decreased by 28%. CP data is reported as an average of triplicate measurements.

#### *Attenuated Total Reflectance Fourier Transform Infrared Spectrometry*

A Thermo Nicolet Nexus 470 spectrometer with wavenumbers ranging from 400 to 4000 $cm^{-1}$, with a deuterated triglycine sulfate pyroelectric detector, was used. Samples were kept for at least 2 hours in glass tubes either

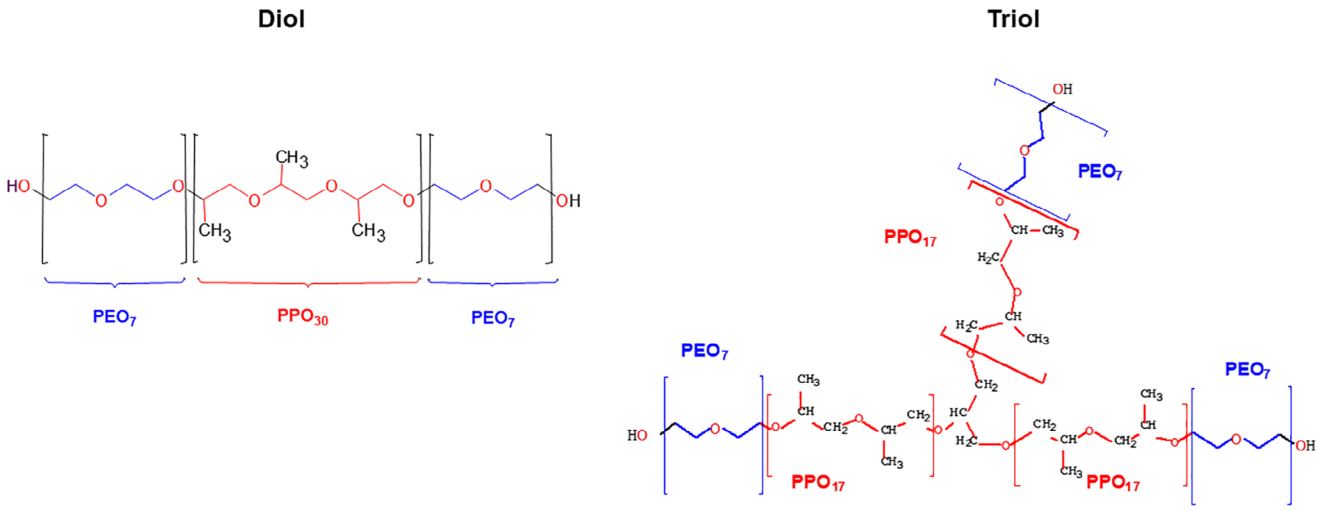


**Fig. 1** Chemical structures of Diol and Triol

at room temperature (24 °C), low temperature (−15 °C), or high temperature (80 °C).

*Small-Angle X-Ray Scattering (SAXS)*

SAXS measurements were performed at a NanoStar SAXS System, by Bruker, with two-dimensional detector. The machine has a microfocus source Genix3D (CuKα wavelength λ = 1.54 Å), Fox3D-focusing mirror, and two sets of scatterless slits, all provided by Xenocs. The obtained 2D images were integrated azimuthally and corrected for sample transmission and solvent scattering. The obtained SAXS data covers a q-range of 0.013–0.33 $Å^{-1}$, where q is the reciprocal space momentum transfer modulus, defined as $q = 4\pi \sin(\theta)/\lambda$, wh ere 2θ is the scattering angle and λ the radiation wavelength. The samples were placed in a glass capillary and the measurements were performed at room temperature with varying concentration and with temperature control at a fixed concentration of 50%.

*Dynamic Light Scattering*

DLS measurements were performed using a Brookhaven 90Plus™ Particle Size Analyzer. The experimental setup is composed of laser beam with wavelength 657 nm and the detector positioned at 90° with respect to the incoming beam. Temporal autocorrelation curves were obtained using standard routines of the acquisition programs. The experiments were performed in homodyne mode. The DLS experiment was performed for samples with 50% Diol/Triol in 25% DB, and temperature ranging from 20 °C to 70 °C.

## SAXS Modeling

Reversed spherical micelles with inner radius polydispersity were modeled, with hard-spheres interaction, by using the Decoupling Approximation. The scattered intensity is given by (Kotlarchyk and Chen, 1983; Pedersen, 1997):

$$I(q) = n_P P(q) S'(q) \tag{1}$$

Where $q = 4\pi\sin\theta/\lambda$ is the modulus of the reciprocal space momentum transfer, with $2\theta$ the scattering angle and $\lambda$ the radiation wavelength $n_P = conc\ N_A/A_G$ is the particle number density with *conc* being polymer concentration (M), $N_A$ the Avogadro's number and $A_G$ the aggregation number. P(q) is the form factor of core-shell reverse spherical micelles, considering that the nuclei of solvent are surrounded by the polymer molecules. Thus, the inner part of the spheres is formed by solvent, surrounded by the hydrophilic shell (PEO), and the medium is formed mainly by the hydrophobic part of the Diol(Triol) (PPO). The form factor is given by (Pedersen, 1997; Teixeira et al., 2010):

$$P(q) = \left\langle \left| \left(F_{core}(q) + F_{shell}(q)\right)^2 \right| \right\rangle \tag{2}$$

Where (Pedersen, 1997)

$$F(q)_{core(shell)} = \frac{4\pi R_{core(shell)}^3}{3}\left(\rho_{medium(shell)}\right) - \rho_{shell(core)} \left(\frac{3\sin\left(qR_{core(shell)}\right) - qR_{core(shell)}\cos\left(qR_{core(shell)}\right)}{\left(qR_{core(shell)}\right)^3}\right) \tag{3}$$

$F_{core(shell)}$ is the scattering amplitude due to the micelles core (the solvent nucleus in this case) or the shell (the hydrophilic region of the polymer).

$R_{core}$ and $R_{shell}$ are, respectively, the core and total radius of the spheres.

$\rho_{medium}$ is the electron density of the matrix (in this case, the PPO segments).

$\rho_{shell}$ is the electron density of the micelles shell, formed by the PEO segments.

$\rho_{core}$ is the electron density of the micelle core, in this case the solvent used (25 dB).

$S'(q)$ is the apparent interparticle structure factor, given by:

$$S'(q) = 1 + \beta(q)[S(q) - 1].$$

The factor β suppresses the oscillations of the true structure factor $S(q)$ due to the polydispersity:

$$\beta(q) = \frac{|\langle F(q)\rangle|^2}{\left\langle |F(q)|^2 \right\rangle} \tag{4}$$

The inner radius was considered to be polydisperse, with Gaussian size distribution:

$$f(r) = \frac{1}{(2\pi\sigma^2)^{1/2}} exp\left[-\frac{(R-\langle R\rangle^2}{2\sigma^2}\right], \tag{5}$$

where σ is the root-mean-square deviation from the mean radius and $\langle R\rangle$ is the average radius.

The above averages are:

$$\left\langle |F(q)|^2 \right\rangle = \int_0^\infty |F(q,r)|^2 f(r) dr \tag{6}$$

and

$$|\langle F(q)\rangle|^2 = \left| \int_0^\infty F(q,r) f(r) dr \right|^2. \tag{7}$$

As the micelles are not charged, we used the Percus Yevick hard-sphere interaction (Kinning and Thomas, 1984):

$$S(q) = \frac{1}{1 + 24\eta(G(A)/A)}, \tag{8}$$

$A = 2qR_{HS}$, $R_{HS}$ is the interaction (hard sphere) radius, and

$$G(A) = \frac{\alpha}{A^2}\left(\sin A - A\cos A\right) + \frac{\beta}{A^3}\left(2A\sin A + (2 - A^2)cosA - 2\right) + \frac{\gamma}{A^5}\left(-A^4 cosA + 4\left[\left(3A^2 - 6\right)cosA + \left(A^3 - 6A\right)\sin A + 6\right]\right) \tag{9}$$

where

$$\alpha = (1+2\eta)^2/(1-\eta)^4 \tag{10}$$

$$\beta = -6\eta(1+\eta_2)^2/(1-\eta)^4 \tag{11}$$

$$\gamma = \frac{(1/2)\eta(1+2\eta)^2}{(1-\eta)^4} \tag{12}$$

and $\eta = 4\pi R^3 n_P/3$ is the hard-sphere volume fraction and $n_P$ is the particle number density.

A fraction of interacting micelles in solution was included in the total scattering intensity, which corresponds to a polydispersity of the interaction radius. Thus, the total intensity was calculated, allowing the possibility of interaction between a fraction of the micelles in solution (Teixeira et al., 2010):

$$I(q) = BG + SF \times P(q)\,(1 + fr\,S'(q)) \tag{13}$$

As the experiments were not performed in absolute scale, we include the term SF = scaling factor, which accounts for the particle number density and the scale differences between the experiment and the absolute unit. BG is a flat background noise. *fr* is the fraction of the micelles that take part in the interaction. The modeled function was written and fitted with the program Igor Pro (WaveMetrics, http://www.wavemetrics.com), version 6.37, using the least-squares method.

The input parameters are:

BG = constant background

SF = overall scaling factor

$R_{core}$(Å) = inner radius = radius of the solvent nucleus

$R_{shell}$(Å) = total radius of the sphere = Rpar + thickness of the polar region

$\rho_{shell}$ = electron density of the polar region (PEO). It was initially calculated from the number of electrons and volume of a PEO chain. This value was used as starting value, which was then left free to be fitted.

$\rho_{core}$ = electron density of the solvent (micelle nucleus). It was calculated from the number of electrons and volume of water and 2-(2-butoxyethoxy) ethanol molecules, weighed by their concentration (75% water:25% 2-(2-butoxyethoxy) ethanol). This value was kept constant during all the fitting procedure.

$\rho_{medium}$ = electron density of the (PPO). It was initially calculated from the number of electrons and volume of a PPO chain, which was used as starting value and then left free to be fitted.

*conc* = solvent concentration (M), as the micelles are reverse

$R_{HS}$ = interaction (hard sphere) radius

$\sigma_{polycore}$ = root-mean-square deviation from the mean radius (of the inner (solvent) radius)

fr = fraction of interacting micelles

As $\rho_{core}$ is known and fixed, the electron densities of the shell and medium are scaled by their contrast with $\rho_{core}$. Therefore, the values are reliable and meaningful.

The concentration of the sample was calculated from the mass percentage of polymer in solution. As the micelles are reverse and the concentration is used to calculate η (volume fraction of hard-spheres), the concentration of solvent in Molar is used as input parameter. The amounts of water (75%) and DB (25%) were considered for the molecular weight calculation. This parameter was kept constant during the fitting procedure.

BG and SF were initially fitted and an average was chosen to be the same constant value for the whole set of curves

$R_{core}$, $R_{shell}$, $\rho_{shell}$, $\rho_{medium}$, $R_{HS}$, $\sigma_{polycore}$ and fr were fitted

From $\sigma_{polycore}$, the inner radius polydispersity was calculated ($\delta_{core} = \sigma_{core}/R_{core}$)

## Results

### Cloud-Point

Initially, the CPs of Diol and Triol in distilled water were determined. The CP in pure water occurred at quite low temperatures (Table 1), indicating very high hydrophobicity of Diol and Triol. To increase the CP, a solution containing 25% of 2-(2-butoxyetoxy) ethanol (ether butyl diglycol) in water was used throughout (25 dB). The CPs of Diol and Triol for concentrations of 3–99% in 25 dB are shown in Table 2. The transmittance curves are shown in Fig. S1. The CP temperature decreases up to concentrations of 25% Diol, where it reaches a minimum, and increases after 35% Diol. At 90% and 95% Diol, the temperature at which the solution transmittance decreased was not sharp; therefore, the values were not presented. For 97%, the CP was not even observed. When the solutions are left at rest for a long time, a phase separation occurs immediately above the CP temperature. The CP temperatures obtained for Triol followed the same trend, and the values were very close for both systems.

### Attenuated Total Reflectance Fourier Transformed Infrared

The ATR-FTIR spectra of polyether glycols Diol and Triol are shown in Fig. S2. The wavenumbers related to the vibrational spectra of the different groups present in the sample were identified: a broad peak between 3100 and 3700 $cm^{-1}$, due to the stretching of the O—H groups from water, 2-(2-butoxyetoxy)ethanol and the hydroxyl groups at the end of the polymer chains; the stretching of the C—O—C of the polyether chains at 1100 $cm^{-1}$; the vibration of the C—H chains; bending vibration of O—H groups at the end of the chains and the hydrogen bond of the water molecule, near 1650 $cm^{-1}$ (Bayly et al., 1963; Shen and Wu, 2003; Zhang et al., 2008b). All these observed regions are in agreement to what is expected for aqueous solutions of PEO-PPO-PEO copolymers (Guo et al., 2000; Jia et al., 2010; Su et al., 2002a, b).

The analysis of the data was qualitatively performed due to the low spectral resolution. The stretching of the C—O groups is known as an indication of micelles formation (Jia et al., 2010; Su et al., 2002b). As the water content is not high, and as the PEO groups have more affinity with water, the hydrophobic PPO chains, which are more abundant in our samples, would tend to be located at the surrounding. Thus, we infer that the micelles in the present system are reverse. No significant difference was observed between Diol and Triol, which is expected, as both have the same groups.

### Dynamic Light Scattering

The results obtained by DLS for Diol showed correlation times in the range of decimals of microseconds from 20 °C

**Table 1** Cloud points of Diol and Triol in distilled water

| Polyether glycol mass % | Cloud point (°C) | |
|---|---|---|
| | Diol | Triol |
| 0.5 | 34.3 | 32.4 |
| 1.0 | 31.4 | 28.7 |
| 2.5 | 27.8 | 25.4 |
| 5.0 | 23.8 | 22.5 |
| 10.0 | 22.3 | 21.3 |

**Table 2** Cloud points of Diol and Triol in 25% of 2-(2-butoxyetoxy) ethanol in water (25 dB)

| Polyeter glycol (Mass %) | Cloud point (°C) | |
|---|---|---|
| | Diol | Triol |
| 3.0 | 73.7 | – |
| 5.0 | 67.8 | 67.1 |
| 10.0 | 59.5 | 58.9 |
| 20.0 | 54.7 | 53.6 |
| 25.0 | 54.9 | 53.1 |
| 35.0 | 54.9 | 54.7 |
| 40.0 | 56.9 | 55.8 |
| 50.0 | 63.6 | 60.5 |
| 60.0 | 68.5 | 64.8 |
| 70.0 | 72.4 | 68.3 |
| 80.0 | 75.0 | 70.0 |
| 90.0 | – | – |
| 95.0 | – | – |
| 97.0 | Not observed | Not observed |
| 98.0 | Not observed | Not observed |
| 99.0 | Not observed | Not observed |
| 99.5 | Not observed | Not observed |

to 55 °C, increasing with temperature, becoming much higher from 60 °C on, reaching units of microseconds. At 70 °C, the correlation curve rises up, indicating the presence of very large particles in solution. The correlation curves for Triol present longer correlation times, which also increase with temperature and become considerably high already at 55 °C, showing that the particles are growing. At 70 °C, the particles are even larger, as the correlation curve moves up. The correlation curves of Diol and Triol for all measured temperatures are shown in Fig. S3.

## SAXS

### *Concentration Dependence*

SAXS curves at room temperature were obtained for polymer concentrations ranging from 5% to 95%, but no intensity was detected for concentrations lower than 40%. Thus, analysis was performed for 50% on. The curves are shown in Fig. 2, in the same arbitrary units for both measurement sets.

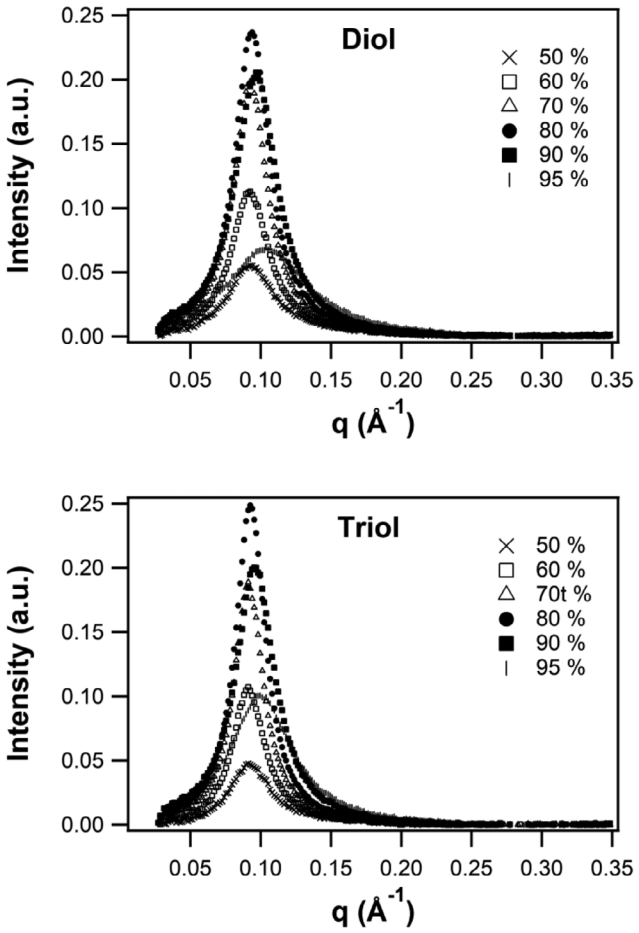


**Fig. 2** SAXS curves for Diol in 25 dB (left) and Triol in 25 dB (right)

For both systems, an increase in intensity is observed between 50 wt% and 80 wt%, where it reaches its maximum value, then decreases and shifts toward higher *q*-values. The intensities at each concentration are close for both systems, except for 95 wt%, which is lower for Diol. As the polymer concentration is very high, reverse micelles were considered. The spherical shape fitted properly the micelles in the system. Attempts to fit the form factor of direct spherical micelles and elongated structures were made, leading to unreasonable parameters (results not shown). Thus, intensity of reverse spherical core-shell micelles with hard-spheres interaction was fitted to the curves, where the PPO hydrophobic segments were considered as the outer medium and the PEO hydrophilic groups as the outer part of the micelles surrounding the inner solvent cores.

The fitting results for Diol and Triol at room temperature are shown in Figs. 3 and 4, respectively, and the fitted parameters in Tables 3 and 4, for Diol and Triol, respectively. The inner micelle radii increase from 50% to 80% of polymer (for both polymers), decreasing at 95%. The core radius is bigger for Triol, for practically all concentrations. The total micelle radius ($R_{shell}$) is almost constant, up to 80%, decreasing at 90% and 95%.

The electron densities of the hydrophilic and hydrophobic segments are very close, but distinguishable within the error bars. Their variation with concentration is shown in Fig. 5. Figure S4 shows the theoretical intensity calculated with the parameters obtained for the sample with 50% Diol, for a core-shell structure, compared to the intensity calculated for homogeneous particles with the same parameters, showing the effect of the small electron density differences. The interaction radius is constant up to 80%, starting to decrease at 90%, for Diol and Triol, being very close to the total radius and, although within the error bars, slightly smaller in some cases. It might happen as the polymer chains are flexible and can be interpenetrated. At 90% and 95%, the fraction of interacting hard-spheres decreases, as little solvent is available. The polydispersity of the core (solvent) radius oscillates, having the highest value at 95%. However, as we do not have enough accuracy to determine how much water there is in the polymer chains, it is not reasonable to speculate about precise radius or polydispersity. Instead, we shall only take the general trend, as to say, at higher polymer concentration, the system tends to be more polydisperse than at lower polymer concentrations. Both systems, Diol and Triol, are very similar at room temperature.

### *Temperature Dependence*

SAXS curves were also obtained for the concentration of 50 wt% of Diol in 25 dB at 25 °C, 50 °C, 60 °C, and 70 °C, and are shown in Fig. 6. As the temperature increases, the oscillation "peak" becomes asymmetrically

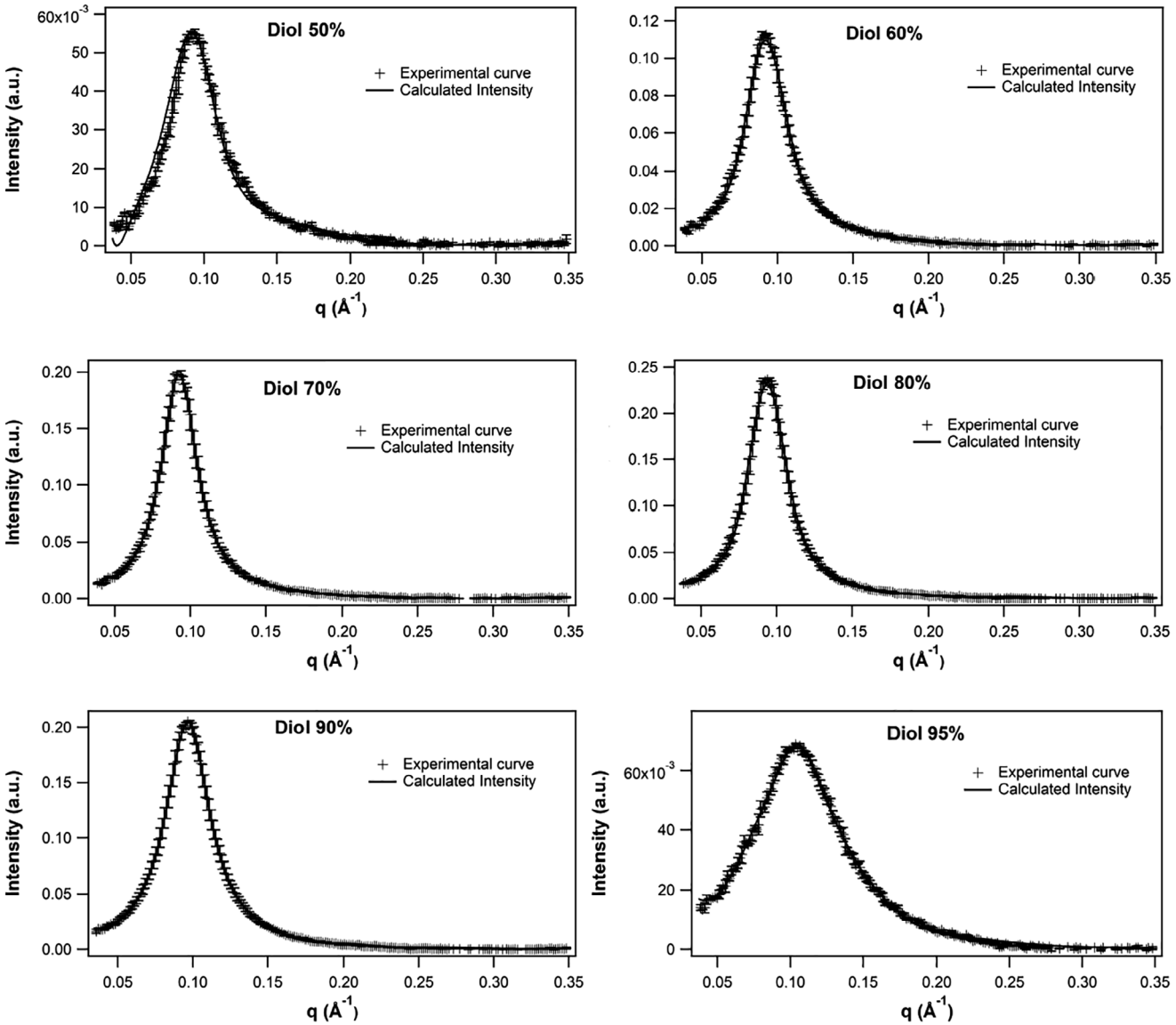


**Fig. 3** SAXS curves of Diol (symbols) with fitted intensities (lines)

broader toward higher q, whereas its maximum is seen almost like a shoulder and moves to lower q-values as the temperature increases.

The fitted curves and the obtained parameters are shown in Fig. 7 and Table 5, respectively. The values of $R_{core}$ and $R_{shell}$ obtained for the temperature-controlled run are higher than those obtained at room temperature, even at 25 °C. As the room temperature was not controlled, it might have been different from 25 °C. Besides, there might also be some fluctuation in concentration, as both series correspond to different sample preparations. Therefore, comparisons are made only among curves belonging to the same set of measurements. As the temperature increases, $R_{core}$ decreases and the interaction radius ($R_{HS}$) increases, whereas $R_{shell}$ does not show any special tendency, having similar values at 25 °C and 70 °C.

The electron densities of the PPO medium and polar region (Table 5 and Fig. 5) are very close. The difference between them become very small at 50 °C and above (see Fig. 5 – bottom). The PEO chains, hydrophobic at higher temperatures, shrank and, for being so short, are close together with the hydrophobic PPO chains. The micelles' shell corresponds to a transition layer between the solvent core the hydrophobic medium, being no longer well-defined. Polidispersity of the solvent core ($\delta_{core}$) is negligible, except at 70 °C.

## Discussion

Diol and Triol have a low PEO:PPO ratio and tend to be quite strongly hydrophobic, reaching the CP at room

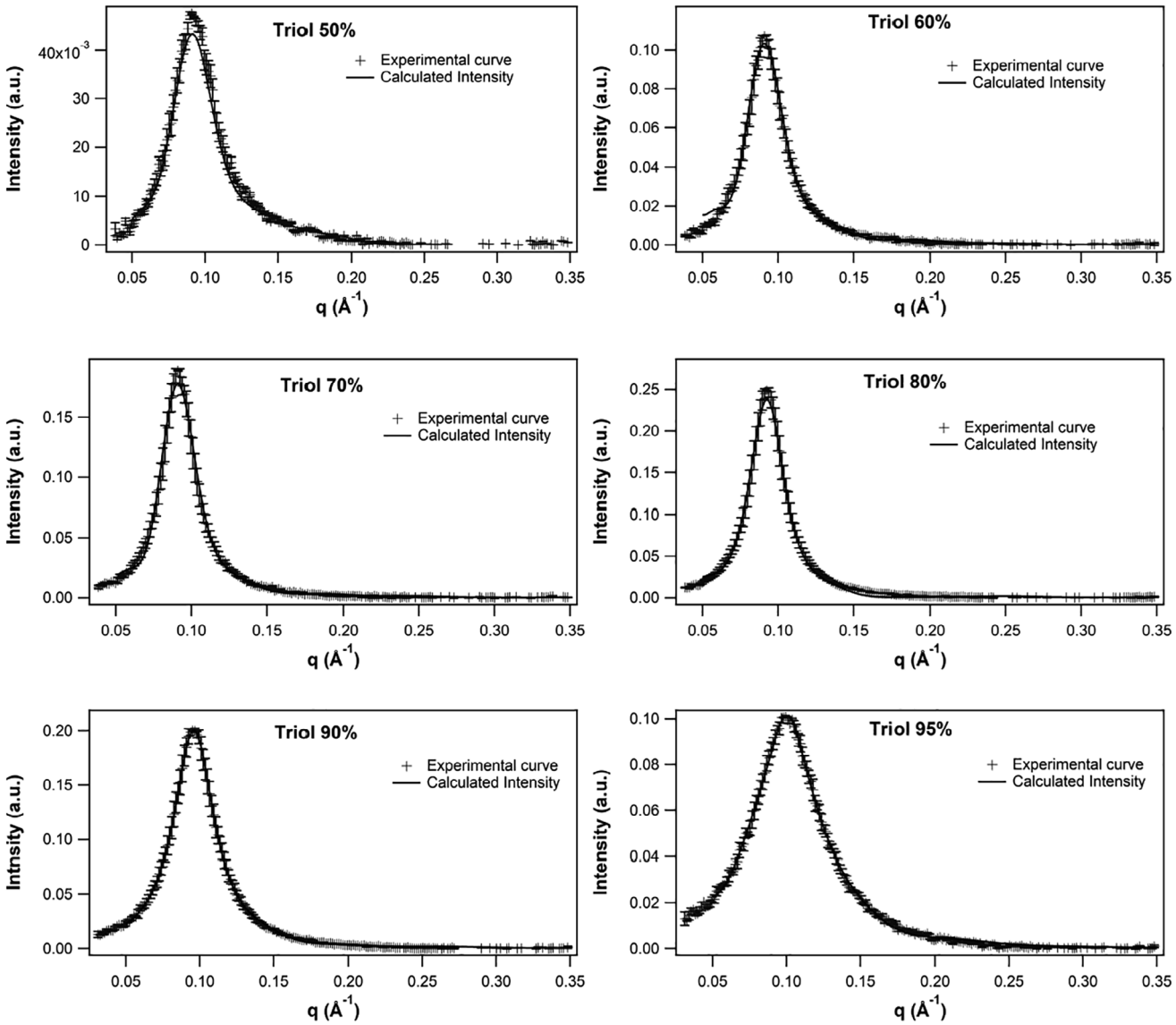


**Fig. 4** SAXS curves of Triol (symbols) with fitted intensities (lines)

**Table 3** Parameters obtained from the fittings of the samples containing Diol in 25 dB at room temperature, at different concentrations

| | 50% | 60% | 70% | 80% | 90% | 95% |
|---|---|---|---|---|---|---|
| $R_{core}$ (Å) | 17.2 ± 0.2 | 17.5 ± 0.5 | 18.2 ± 0.2 | 18.0 ± 0.2 | 18.6 ± 0.1 | 14.1 ± 0.1 |
| $R_{shell}$ (Å) | 59 ± 1 | 60.6 ± 0.3 | 60.7 ± 0.5 | 60.0 ± 0.5 | 56 ± 1 | 49 ± 1 |
| $\rho_{shell}$ (el/Å$^3$) | 0.3511 ± 0.0008 | 0.3557 ± 0.0002 | 0.3570 ± 0.0002 | 0.3615 ± 0.0001 | 0.3604 ± 0.0002 | 0.3690 ± 0.0002 |
| $\rho_{medium}$ (el/Å$^3$) | 0.3500 ± 0.0001 | 0.3539 ± 0.0001 | 0.3539 ± 0.0002 | 0.3585 ± 0.0002 | 0.3584 ± 0.0002 | 0.3676 ± 0.0002 |
| $R_{HS}$ (Å) | 60 ± 1 | 60 ± 1 | 60 ± 1 | 59 ± 1 | 58 ± 1 | 54 ± 1 |
| $\delta_{core}$ | 0.109 ± 0.017 | 0.120 ± 0.017 | 0.143 ± 0.006 | 0.139 ± 0.017 | 0.134 ± 0.016 | 0.191 ± 0.014 |
| fr | 1 | 1 | 1 | 1 | 0.9 ± 0.1 | 0.3 ± 0.1 |

$R_{core}$, inner radius (inner solvent core); $R_{shell}$, total radius, including the hydrophilic radius; $\rho_{shell}$, electron density of the hydrophilic (PEO) part; $\rho_{medium}$, electron density of the hydrophobic medium (PPO); $R_{HS}$, interaction radius; $\delta_{core}$, polydispersity; fr, fraction of interacting micelles; $\rho_{core}$, 0.333 electrons/Å$^3$.

**Table 4** Parameters obtained from the fittings of the samples Triol in 25 dB at temperature, at different concentrations

| | 50% | 60% | 70% | 80% | 90% | 95% |
|---|---|---|---|---|---|---|
| $R_{core}$ (Å) | 17.1 ± 0.1 | 18.7 ± 0.2 | 21.0 ± 0.3 | 20.7 ± 0.2 | 20.1 ± 0.1 | 15.4 ± 0.1 |
| $R_{shell}$ (Å) | 60.1 ± 0.3 | 61.6 ± 0.4 | 61.0 ± 0.3 | 61.0 ± 0.5 | 56 ± 1 | 51.8 ± 0.5 |
| $\rho_{shell}$ (el/Å$^3$) | 0.34675 ± 0.00005 | 0.3500 ± 0.0001 | 0.3497 ± 0.0001 | 0.3539 ± 0.0001 | 0.3572 ± 0.0001 | 0.3650 ± 0.0001 |
| $\rho_{medium}$ (el/Å$^3$) | 0.34550 ± 0.00005 | 0.3480 ± 0.0001 | 0.3470 ± 0.0001 | 0.3510 ± 0.0001 | 0.3557 ± 0.0001 | 0.3633 ± 0.0001 |
| $R_{HS}$ (Å) | 61 ± 1 | 61 ± 1 | 61.1 ± 0.5 | 60 ± 1 | 59 ± 1 | 56.2 ± 0.7 |
| $\delta_{core}$ | 0.175 ± 0.012 | 0.123 ± 0.011 | 0.133 ± 0.005 | 0.097 ± 0.005 | 0.060 ± 0.005 | 0.188 ± 0.007 |
| fr | 1 | 1 | 1 | 1 | 0.76 ± 0.03 | 0.30 ± 0.05 |

$R_{core}$, inner radius (inner solvent core); $R_{shell}$, total radius; including the hydrophilic radius; $\rho_{shell}$, electron density of the hydrophilic (PEO) part; $\rho_{medium}$, electron density of the hydrophobic medium (PPO); $R_{HS}$, interaction radius; $\delta_{core}$, polydispersity; fr, fraction of interacting micelles. $\rho_{core}$, 0.333 electrons/Å$^3$.

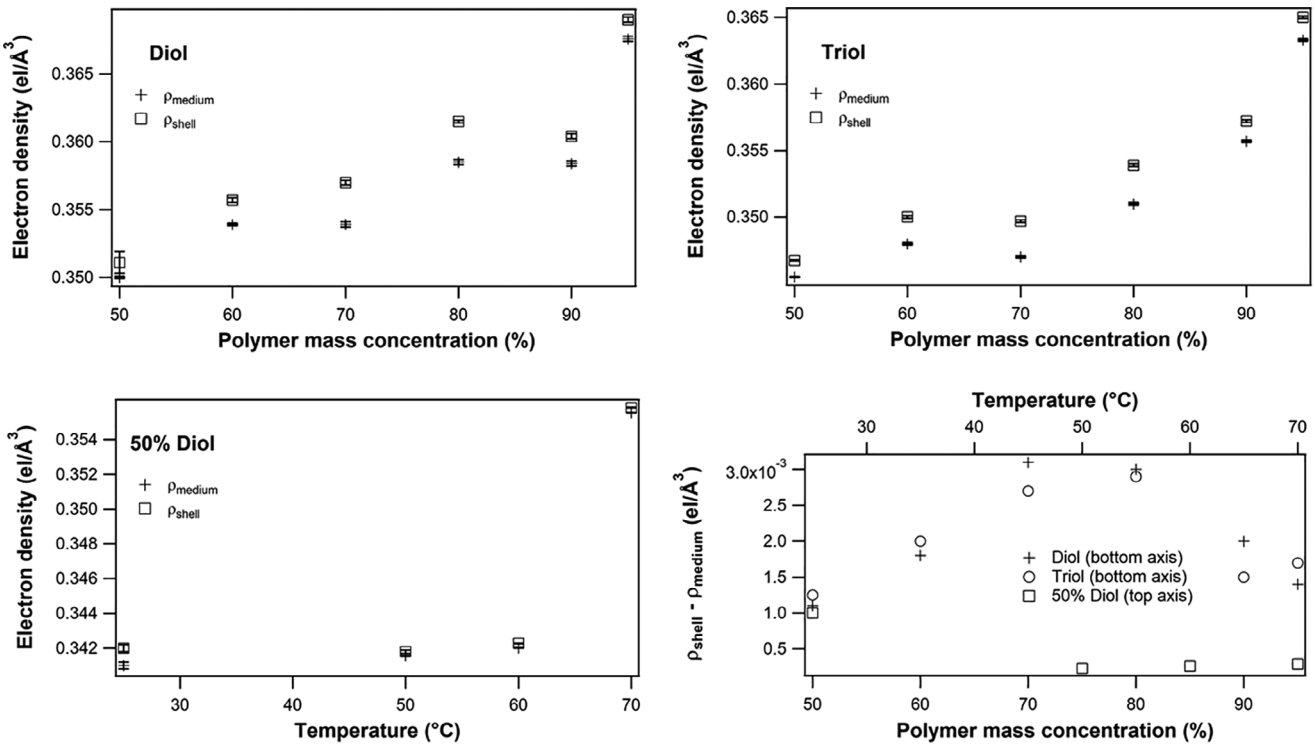


**Fig. 5** Electron densities of: Diol, with concentration (left, up); Triol, with concentration (right, up); 50% Diol with temperature (left, bottom); difference between $\rho_{shell}$–$\rho_{medium}$ for Diol and Triol for different concentration and 50% Diol for different temperatures (right, bottom)

temperature at 10% in water. The addition of 25% of the glycol ether butyl diglycol (DB) to water considerably increases their hydrophilicity and consequently their CP up to 75 °C (Diol) and 70 °C (Triol) at 80%, allowing the presence of micelles in solution up to very high copolymer concentrations, preventing turbidity and phase separation. CP of Triol is close to, but always lower, than Diol. Herfurth et al. (2016) also observed lower CP for star-like copolymers in comparison to linear copolymers. The structures (micelles and ordered structures) formed by triblock copolymers depend on the copolymer structure, on the PEO:PPO ratio and the solvent quality. The low PEO:PPO ratio favors the formation of micelles with negative curvature (reverse, with curvature toward the polar part). Pluronic L92 ($EO_8PO_{47}EO_8$) and Pluronic L122 ($PEO_{11}PPO_{70}PEO_{11}$) also formed reverse structures in aqueous solution (Svensson et al., 1999) at high polymer concentrations, although direct micelles were observed at low concentrations. But both L92 and L122 have longer PPO chains than Diol and Triol, which most affects the micelle formation.(Alexandridis et al., 1994) Here, the shorter PPO chains favored the negative curvature. Besides, non-polar solvents, with strong tendency to swell the PPO chains, are able to promote the formation of reverse

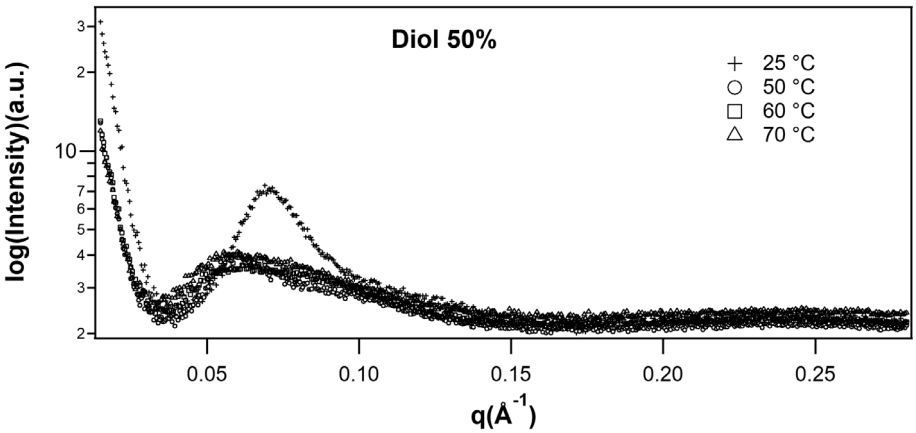


**Fig. 6** SAXS curves obtained for 50% Diol in 25 dB at different temperatures

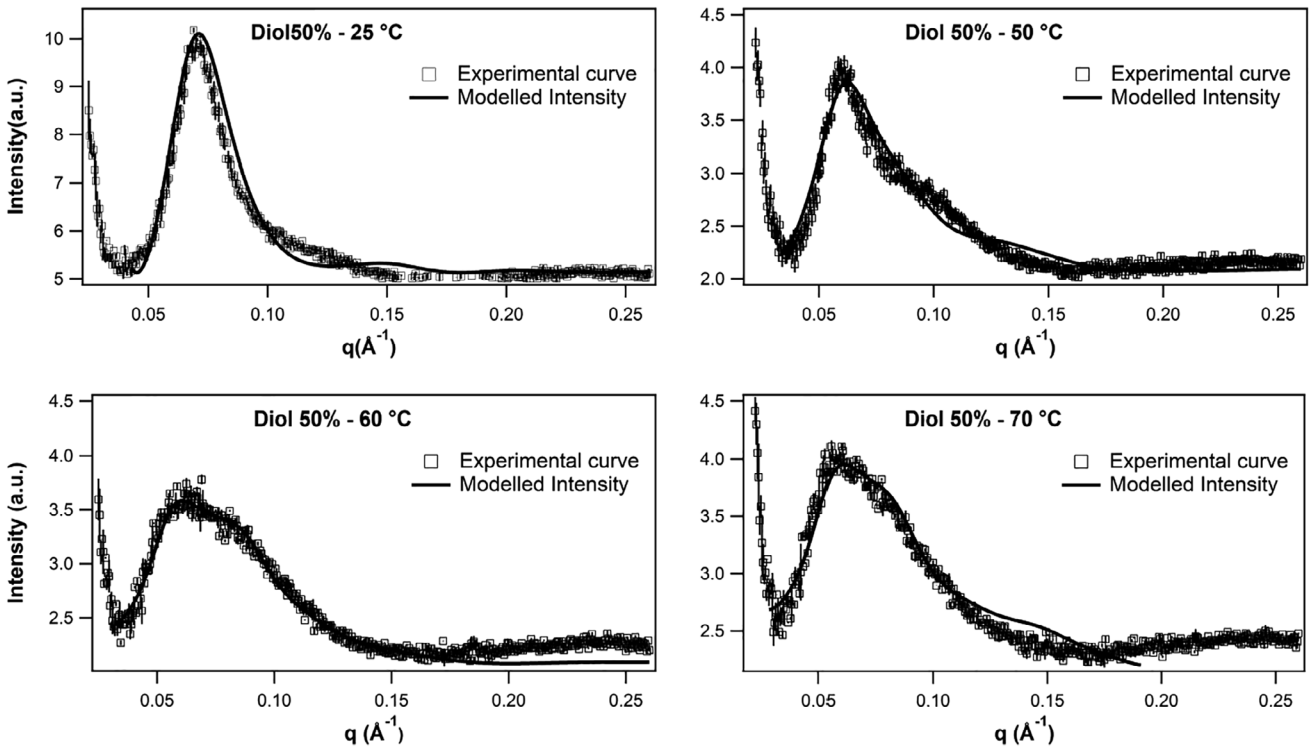


**Fig. 7** SAXS curves (symbols) of 50% Diol in 25 dB at different temperatures, along with fitted intensities (lines)

structures (Svensson et al., 1998). Especially, the mixture of a PPO resembling solvent in water increases the miscibility of the whole molecule, being the reason why micelles were not observed at concentrations as high as 30 wt%, as the whole molecule is well hydrated. When the copolymer concentration increases, PPO becomes hydrophobic, segregation between PEO and PPO chains occurs, and the micelles are formed. At this high concentration, the short PEO chains promote the formation of reverse micelles.

The variation of the three radii ($R_{core}$, $R_{shell}$, and $R_{HS}$) with polymer concentration can be easily followed in Fig. 8, for Diol and Triol. Starting from the highest polymer concentration, decreasing from 95% to 80% the small cores formed mainly by solvent increase when the amount of solvent increases, accompanied by an increase in the interaction radius. With further increase in solvent concentration (decreasing polymer concentration from 70% to 50%), the micelles radius slightly decreases, whereas the interaction radius is almost constant. As more solvent is present one would, in principle, expect the solvent radius to increase. However, the chains have flexibility to be loose or more compact, and can be shrunk or more extended, depending

**Table 5** Parameters obtained from the fittings of the sample 50% Diol in 25 dB at different temperatures

| | 25 °C | 50 °C | 60 °C | 70 °C |
|---|---|---|---|---|
| $R_{core}$ (Å) | 0 | 22.0 ± 0.3 | 22.3 ± 0.3 | 13.6 ± 0.1 |
| $R_{shell}$ (Å) | 78 ± 1 | 84 ± 1 | 71 ± 2 | 77 ± 1 |
| $\rho_{shell}$ (el/Å$^3$) | 0.3420 ± 0.0002 | 0.3418 ± 0.0001 | 0.34227 ± 0.00001 | 0.35584 ± 0.00002 |
| $\rho_{medium}$ (el/Å$^3$) | 0.3410 ± 0.0002 | 0.34157 ± 0.00002 | 0.34201 ± 0.00001 | 0.35555 ± 0.00002 |
| $R_{HS}$ (Å) | 81 ± 3 | 95 ± 4 | 100 ± 3 | 105 ± 2 |
| $\delta_{core}$ | xx | xx | xx | 0.291 ± 0.003 |
| fr | 1 | 1 | 1 | 1 |

$R_{core}$, inner radius (inner solvent core); $R_{shell}$, total radius; including the hydrophilic radius; $\rho_{shell}$, electron density of the hydrophilic (PEO) part; $\rho_{medium}$, electron density of the hydrophobic medium (PPO); $R_{HS}$, interaction radius; $\delta_{core}$, polydispersity; fr, fraction of interacting micelles. The items marked as xx are negligible (error higher than the corresponding value); $\rho_{core}$, 0.333 electrons/Å$^3$.

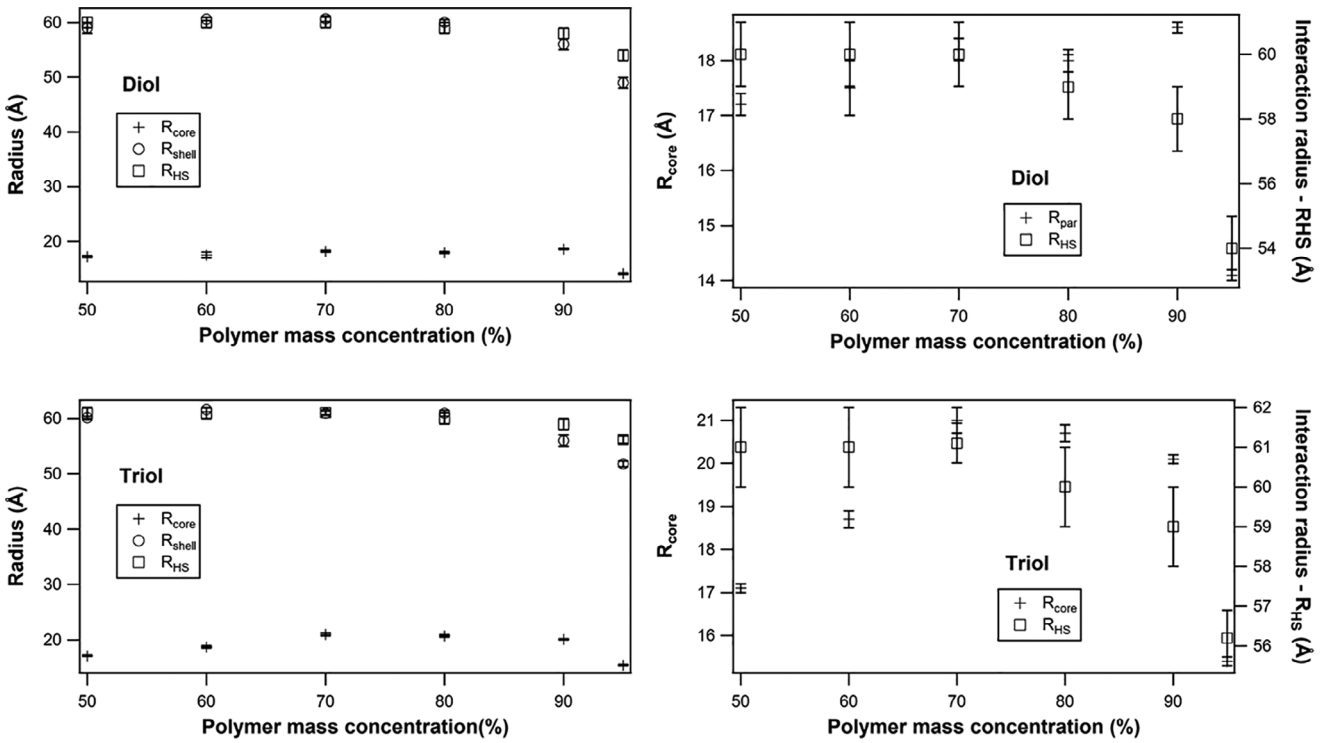


**Fig. 8** Left. Core, total and interaction radii as a function of polymer concentration right. Core and interaction radii as a function of concentration. Up, Diol; bottom, Triol

on the hydration they are exposed to, and also on their hydrophobicity, which depends on the solvent conditions (presence of ions, temperature, co-solvents). At 50% of polymer, there might still be a certain amount of solvent hydrating the corona chains and even the PPO chains, which should be swollen. As the polymer concentration increases to 70–80%, the solvent is gradually expelled from the chains, which shrink, resulting in a slightly higher inner radius, while the distance between centers remains practically constant, with more compact chains. Above 80%, there is too little solvent in the sample, so the inner radius decreases and the chains shrink further, shortening the distance between solvent spheres. The chains shrinkage is in agreement with the increase in their electron density, observed in Tables 3 and 4 and Fig. 5. The increasing difference between the electron densities of the PPO medium and the shell with increasing concentration also shows a gradual separation of the shell and the highly dehydrated medium: from well hydrated polymer when micelles start to be well observed at 50% until complete dehydration of the medium when the concentration increases and the solvent is expelled. SAXS curves for 100% Diol and 100% Triol showed the features of core-shell structure and could only be fitted with two-electron density spheres, clearly

indicating a separation of the PEO and PPO chains (Fig. S5). Segregation of different parts of block copolymers and the decrease in the amount of solvent in the hydrophobic segments have already been observed by other authors (Etampawala et al., 2016). A decrease in the fraction of interacting micelles from unity for the highest concentrations suggests that the cores are not equally distributed in the sample volume.

**Temperature Dependence**

The PPO blocks are more hydrophobic, and responsible for the micelles formation (Alexandridis et al., 1994) at a constant concentration, when the temperature increases. At moderate temperature, the PEO groups are hydrophilic, but its hydrophilicity decreases as the temperature increases and both blocks become more hydrophobic (Holmberg et al., 2002). Then, the polymer region grows fast and finally phase separates from the aqueous phase at the CP. The core radius decreases when the temperature increases (Table 5). The total radius varies without any particular tendency. The tiny difference between the electron densities of the PEO and PPO chains (Fig. 5) become even smaller at higher temperatures, making it hard to distinguish the interface between these two regions. The increase in the electron densities with the temperature indicates a shrinkage of the chains due to dehydration. The interaction radius increases at higher temperatures, showing the formation of big polymer domains separating the small solvent nuclei, which become farther apart from each other.

Our samples were neither viscous nor birefringent, as usually expected for high concentrations and/or high temperatures (Agrawal et al., 2007; Chaibundit et al., 2007; Israelachvili et al., 1976; Lobry et al., 1999; Park and Char, 2004; Tew et al., 2005; Zhang et al., 2007, 2008a), indicating that neither ordered nor liquid crystalline phases were formed. Phase transition concentration and temperature depend on the combination of the PPO size and the PEO:PPO sizes ratio. Several works observed ordered phases of block copolymers in aqueous solution (Chaibundit et al., 2007; Israelachvili et al., 1976; Lobry et al., 1999), but the polymers reported have longer hydrophobic and much longer hydrophilic chains than Diol. Viscous solutions have also been obtained (Chaibundit et al., 2007), even at low polymer concentration (Herfurth et al., 2016), and usually when ordered phases are present (Ghaouar et al., 2016), for copolymers with longer chains, especially long PEO chains.

Gel phase formation and CP strongly depend on the sizes and relative ratios of PPO and PEO chains. Diol has short PPO chain size (30 monomeric units) and extremely short PEO (two chains with 7 units). The PEO:PPO ratios are 0.47 for Diol and 0.41 for Triol. The polymers studied in the cited works have much higher PEO:PPO ratios. Whereas PPO size mainly affects the micelle formation (cmc and cmt) (Alexandridis et al., 1994), the CP is mainly affected by the size of the PEO chains, which, in our case, is smaller than all of the cited copolymers. Such small PEO chains are responsible for the low CP of Diol (22.3 °C) and Triol (21.3 °C) in water at 10%. The 25 DBD increases the CP to 59.5 °C for Diol and 58.9 °C for Triol, at 10%, as the solvent can easily penetrate the PEO and PPO regions. The good hydration of the whole molecule and the low PPO and PEO contents in the molecule, is probably responsible for the absence of an ordered or gel phase, when the concentration increases. The formation of reverse micelles can also be inferred by the increase in the CP at 40% and higher polymer concentrations (Table 2), that happens for both, Diol and Triol. From this concentration on, as the amount of solvent in the system decreases, the CP only increases. In systems containing direct micelles, the micelles sizes increase with temperature, becoming very big near the CP. In this case, as the micelles cores are formed by the solvent, their size decreases, becoming much smaller at 70 °C, at the same time that the interaction radius, $R_{HS}$, increases (Table 5). It means that the polymer domain surrounding the solvent cores increases. The increasing electron densities of the chains suggests that they are more compact with water expulsion and occupy more space (decrease in solvent core radius) and one can dare to think of an equivalence to a phase separation, as the solvent cores are further apart. The separation between polymer and solvent might occur non-homogeneously within the sample, creating different core sizes and distances, which can cause a poor fitting quality of the curves for intermediate q-values.

As the PPO chains form the medium outside the solvent cores, they are entangled in an almost solvent free medium, and the samples are not viscous, except at the CP. In the work of Chaibundit et al. (2007) the viscous phase is due to the entanglement of the chains in the water medium. Pure (100%) Diol and Triol are gels, but the sample studied with temperature variation at the present work is at 50%, in a PPO-friendly solvent. Some ocular observations were made in samples at 10% and 50% Diol, in solvents containing pure water, 5% of 2-(2-butoxyetoxy)ethanol (5DB), 10% 2-(2-butoxyetoxy)ethanol (10 dB) e 25% 2-(2-butoxyetoxy) ethanol (25 dB), that were heated with a loose temperature control. At 10% Diol, increasing contents of glycol in water makes the samples more homogeneous and increase the temperature at which it becomes turbid. On the other hand, the sample with 50% Diol is isotropic and homogeneous even in pure water. This might be because the micelles are reverse at 50% and the matrix medium is formed by (still hydrated) polymer. In 25 dB all samples were isotropic, non-birefringent, at all temperatures just below the CP. Fig. 9 illustrates the trend of the changes that take place in the system with

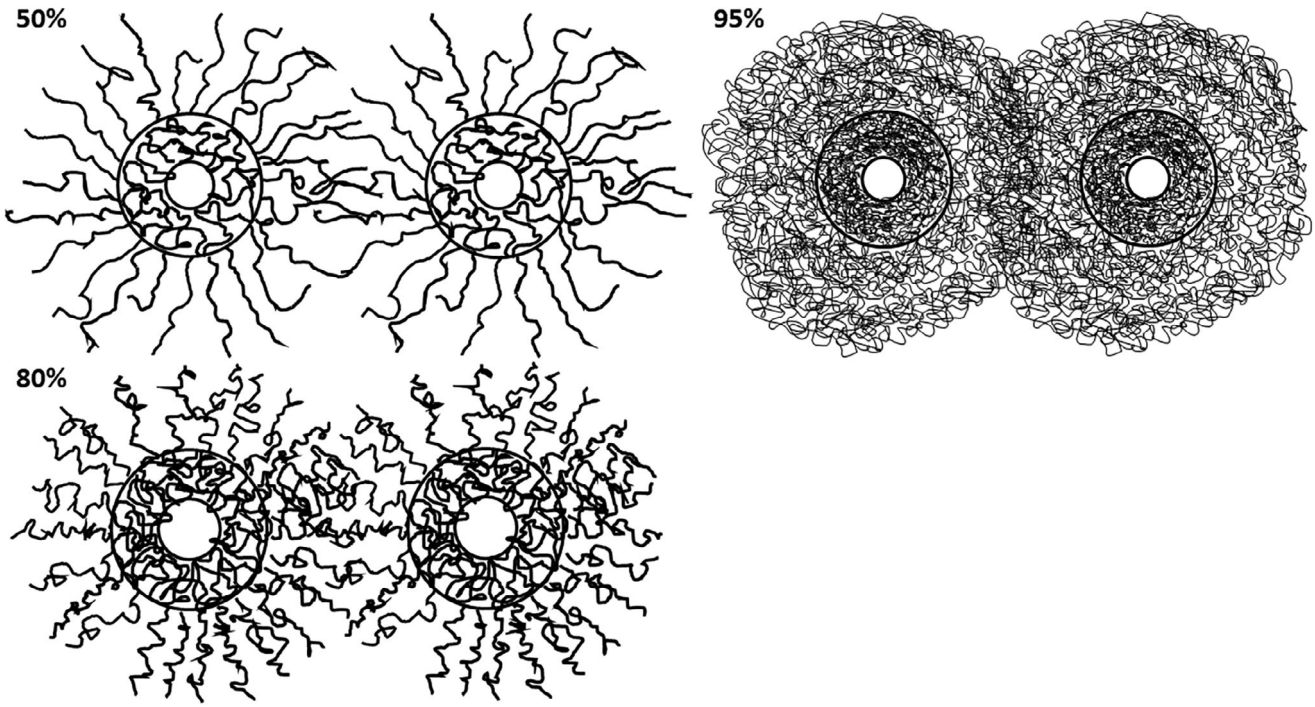


**Fig. 9** Schematic illustration of the structural features of the copolymers in 25 dB at different concentrations. Left up: 50%; left bottom: 80%; right up: 95%

concentration variation. At 50% of polymer the chains are well hydrated, with well extended PPO chains forming the medium around solvent cores. As the solvent is present all over the system, the inner solvent cores are small. As the concentration increases up to 80%, the solvent is expelled from the hydrophobic medium, increasing the size of the inner core, and the flexible chains shrink, keeping the distance between solvent cores unchanged. At extremely high polymer concentration (90% and 95%), there is too little solvent in the system, so that the micelles cores become very small, the polymer chains shrink further and the distance between micelles decreases. Fig. 10 illustrates the structural changes in the system as a function of temperature, at a constant polymer concentration of 50%. From 25 °C to 60 °C, the cores and total micellar radius decrease slightly and the main change is the increase in the distance between solvent cores. The space between the cores is filled by the polymer chains. At 70 °C, the solvent cores are very small and farther apart, with a higher polymer amount occupying the space between the cores.

Karlström calculated the phase diagram of the PEO-water system by using Flory-Huggins theory and concluded that the peculiar behavior of the triblock copolymers in increasing temperatures is a consequence of modifications in the PEO structure as a function of temperature changes and that different conformations of the polymer promote different interaction with the solvent (Karlstrom, 1985). Another model proposes that the local structure of the solvent changes with temperature (Kjellander, 1982; Kjellander and Florin, 1981). Later on, Lindman and Karlström concluded that it is not possible to determine which of the above proposed models can explain the behavior observed experimentally (Lindman and Karlstrom, 2009) and possibly both mechanisms might occur. However, conformational changes of PEO chains, from more polar at low temperature to less polar at high temperature were observed by NMR already in the 70s (Viti and Zampetti, 1973). Nevertheless, all the results converge to the fact that PEO chains are hydrophilic at low temperatures and dehydrate and shrink at high temperature. It is known that addition of alcohol to water modifies its local structure (Nishikawa et al., 1987). It is far beyond the scope of this work to study the theoretical origin of the change in the miscibility of the polymers, but the water–water and water-polymer interactions might have been modified by the presence of the 2-(2-butoxyetoxy) ethanol. Short chain alcohols like ethanol and methanol are also very good solvents for block copolymers, but they suppress the formation of micelles and the CP (Parekh et al., 2012). In addition, the increasing hydrophobicity of the PPO chains and defined separation between the different chains when the polymer concentration increases might be caused by the competition between polymer-solvent and polymer-polymer interactions, being the last one favored when the number of polymer chains is higher than solvent molecules.

Thus, the use of a solvent which has affinity for both parts of the polymer, together with a particularly small

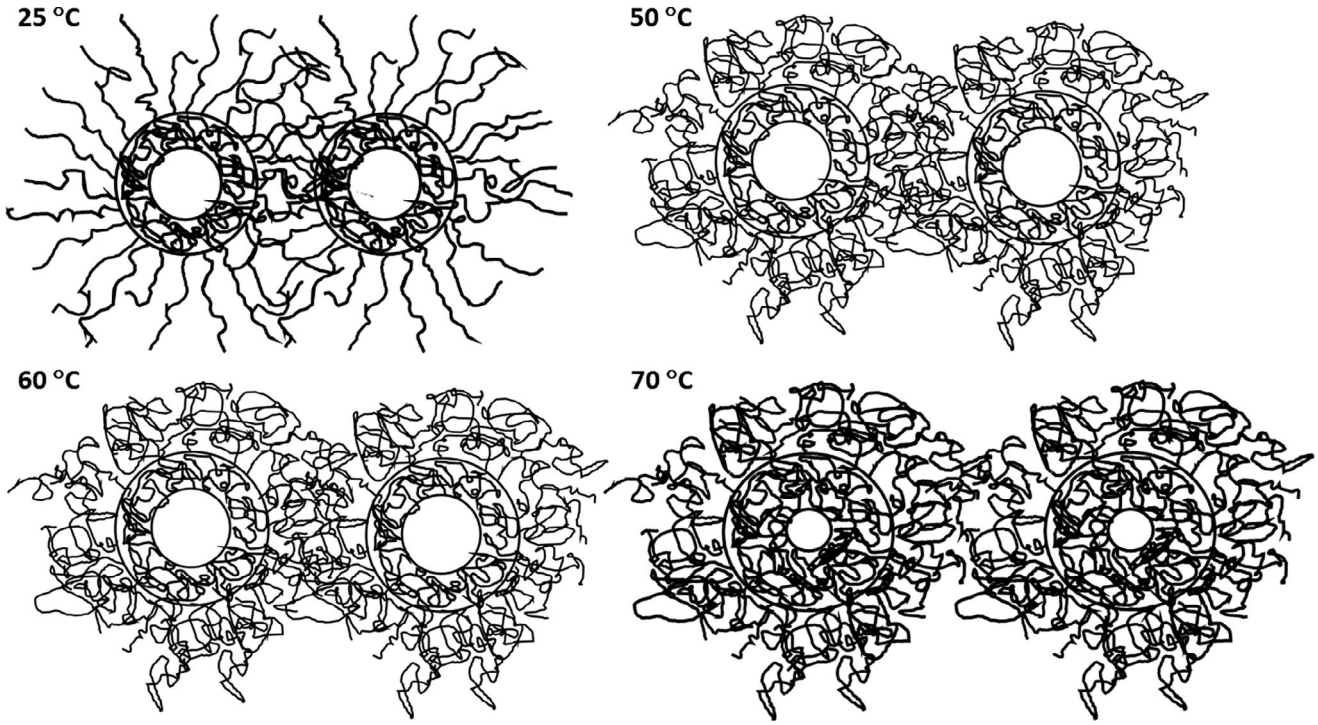


**Fig. 10** Schematic illustration of the structural features of the 50% Diol in 25 dB at different temperatures. Up left: 25 °C; up right: 50 °C; bottom left: 60 °C; bottom right: 70 °C

PEO chain, increased the CP, at the same time it prevented the formation of gel and viscous phase and precipitation for the highly concentrated system.

The aim of the present work was to characterize the structural behavior of the two block copolymers in the presence of a solvent containing water and dibutyl diglycol. Micelles were only observed for high polymer concentrations, small structural changes occurred between 50% and 95% of polymer in solution at room temperature, no ordered phases were formed and the samples were not viscous. Deeper structural changes occur near the CP. The CP, in 25 dB, increases with concentration above 50%. The control of the sizes and viscosity is important in the production of structures for drug delivery (Cambon et al., 2014). 25 dB narrows the CP temperature range, favoring the quality control of the polyether glycol, in a way of certify its composition (Schönfeldt, 1969).

## Conclusions

The structure of Diol and Triol micelles in an aqueous solution of 25% dibutyl diglycol at room temperature was characterized for high polymer concentrations, and also for a mass concentration of 50%, at different temperatures, until the CP. The short hydrophilic and hydrophobic chains of the linear (Diol) and the star-like (Triol) block copolymers make both practically immiscible in pure water, with consequent precipitation at low temperatures, even at low concentrations. The solvent containing 25% of 2-(2-butoxyetoxy) ethanol in water is miscible with both copolymers at all polymer concentrations ranging from 5 to 95%, at room temperature. Above 40% the PPO chains become hydrophobic and reverse micelles are formed. The higher the concentration, the more hydrophobic are the PPO chains, which gradually expel the solvent that will form the cores, surrounded by the hydrophilic PEO chains. At very high polymer concentration (above 80%) the amount of solvent is too small and the PPO chains are completely dehydrated. At this stage, when more polymer is added to the system, the size of the solvent nuclei decreases. At the limit of pure polymer sample, a structure of segregated hydrophilic PEO inside the hydrophobic PPO medium is formed.

As expected, the hydrophobicity increases with temperature. In pure water, the CP is reached at room temperature for 10 wt% of polymer. As the 25 dB has affinity for both regions of the copolymers, the CP increases, and the polymer is present in solution without precipitation, at the whole concentration range at room temperature. Above 40 wt% (Table 2) of polymer in solution, with the formation of reverse micelles, the CP decreases. But the segregation process, with increasing temperature, also occurs at

this concentration: the polymer region increases, and the solvent nuclei decrease in size and get further apart. As the solvent nuclei were already well separated from each other, the phase separation does not form a single solvent phase, as it usually occurs at the lower concentrations normally studied in other systems.

As a consequence of the short hydrophobic segments, responsible for the micelles formation, and the high affinity of both polymers with 25 dB, no ordered phase is formed, despite the high concentrations and temperature increase. Higher amounts of the glycol in water promote the miscibility of higher polymer concentrations, and at higher temperatures. The miscibility of 25% glycol: 75% water with the polymers at room temperature in all concentration range is important for commercial use.

The linear and star-like polymers with similar PEO and PPO contents have very similar behavior in a polar solvent system, except for the slightly lower CP for Triol. This might be because the PEO chains are more exposed to the solvent in Triol, as they are more spread than in Diol.

Metalworking, foam control, structures for drug carrier and delivery, stabilization of cubosomes and hexoxomes and all other applications that rely on their solution behavior can be benefited from the present results.

**Acknowledgements** Thanks are due to FAPESP and CNPq for the financial support and Dow Chemical for providing the materials for the study. MCAF and CLPO are CNPq fellows.

**Conflict of Interest** The authors declare that they have no conflict of interest.

## References

Agrawal, S. K., Sanabria-DeLong, N., Jemian, P. R., Tew, G. N., & Bhatia, S. R. (2007) Micro- to nanoscale structure of biocompatible PLA-PEO-PLA hydrogels. *Langmuir*, **23**:5039–5044.

Akinshina, A., Walker, M., Wilson, M. R., Tiddy, G. J. T., Masters, A. J., & Carbone, P. (2015) Thermodynamics of the self-assembly of non-ionic chromonic molecules using atomistic simulations. The case of TP6EO2M in aqueous solution. *Soft Matter*, **11**:680–691.

Alexandridis, P. (1997) Poly(ethylene oxide) poly(propylene oxide) block copolymer surfactants. *Current Opinion in Colloid & Interface Science*, **2**:478–489.

Alexandridis, P., & Andersson, K. (1997) Reverse micelle formation and water solubilization by polyoxyalkylene block copolymers in organic solvent. *Journal of Physical Chemistry B*, **101**:8103–8111.

Alexandridis, P., & Hatton, T. A. (1995) Poly(ethylene oxide)-poly (propylene oxide)-poly(ethylene oxide) block-copolymer surfactants in aqueous-solutions and at interfaces – Thermodynamics, structure, dynamics, and modeling. *Colloids and Surfaces A-Physicochemical and Engineering Aspects*, **96**:1–46.

Alexandridis, P., & Holzwarth, J. F. (1997) Differential scanning calorimetry investigation of the effect of salts on aqueous solution properties of an amphiphilic block copolymer (Poloxamer). *Langmuir*, **13**:6074–6082.

Alexandridis, P., Holzwarth, J. F., & Hatton, T. A. (1994) Micellization of poly(ethylene oxide)-poly(propylene oxide)-poly (ethylene oxide) triblock copolymers in aqueous-solutions – Thermodynamics of copolymer association. *Macromolecules*, **27**: 2414–2425.

Alexandridis, P., Olsson, U., & Lindman, B. (1996) A reverse micellar cubic phase. *Langmuir*, **12**:1419–1422.

Alexandridis, P., Olsson, U., & Lindman, B. (1998) A record nine different phases (four cubic, two hexagonal, and one lamellar lyotropic liquid crystalline and two micellar solutions) in a ternary isothermal system of an amphiphilic block copolymer and selective solvents (water and oil). *Langmuir*, **14**:2627–2638.

Allen, C., Maysinger, D., & Eisenberg, A. (1999) Nano-engineering block copolymer aggregates for drug delivery. *Colloids and Surfaces B-Biointerfaces*, **16**:3–27.

Bajouk, B. M., & Skold, R. O. (2003) Association and solubility studies of mixed polyglycol ether surfactants in water. *Colloids and Surfaces A: Physicochemical and Engineering Aspects*, **212**:65–77.

Bayly, J. G., Kartha, V. B., & Stevens, W. H. (1963) The absorption spectra of liquid phase H2O, HDO and D2O from 0.7 mu-m to 10 mu-m. *Infrared Physics*, **3**:211–222.

Booth, C., & Attwood, D. (2000) Effects of block architecture and composition on the association properties of poly(oxyalkylene) copolymers in aqueous solution. *Macromolecular Rapid Communications*, **21**:501–527.

Brown, W., Schillen, K., Almgren, M., Hvidt, S., & Bahadur, P. (1991) Micelle and gel formation in a poly(ethylene oxide) poly(propylene oxide) poly(ethylene oxide) triblock copolymer in water solution – Dynamic and static light-scattering and oscillatory shear measurements. *Journal of Physical Chemistry*, **95**: 1850–1858.

Brown, W. L. (1994) Polyalkylene glycols. In *Handbook of lubrication and tribology* (Vol. **III**). Boca Raton, FL: CRC Press LLC.

Cambon, A., Figueroa-Ochoa, E., Juarez, J., Villar-Alvarez, E., Pardo, A., Barbosa, S., … Mosquera, V. (2014) Complex self-assembly of reverse poly(butylene oxide)-poly(ethylene oxide)-poly(butylene oxide) triblock copolymers with long hydrophobic and extremely lengthy hydrophilic blocks. *Journal of Physical Chemistry B*, **118**:5258–5269.

Chaibundit, C., Ricardo, G., Costa, V., Yeates, S. G., & Booth, C. (2007) Micellization and gelation of mixed copolymers P123 and F127 in aqueous solution. *Langmuir*, **23**:9229–9236.

Chaisalee, R., Soontravanich, S., Yanumet, S., & Scamehorn, J. F. (2003) Mechanism of antifoam behavior of solutions of nonionic surfactants above the cloud point. *Journal of Surfactants and Detergents*, **6**:345–351.

Chu, B. (1995) Structure and dynamics of block-copolymer colloids. *Langmuir*, **11**:414–421.

Davaran, S., Ghamkhari, A., Alizadeh, E., Massoumi, B., & Jaymand, M. (2017) Novel dual stimuli-responsive ABC triblock copolymer: RAFT synthesis, "schizophrenic" micellization, and its performance as an anticancer drug delivery nanosystem. *Journal of Colloid and Interface Science*, **488**:282–293.

Desai, P. R., Jain, N. J., Sharma, R. K., & Bahadur, P. (2001) Effect of additives on the micellization of PEO/PPO/PEO block copolymer F127 in aqueous solution. *Colloids and Surfaces A-Physicochemical and Engineering Aspects*, **178**:57–69.

Dormidontova, E. E. (2004) Influence of end groups on phase behavior and properties of PEO in aqueous solutions. *Macromolecules*, **37**:7747–7761.

Etampawala, T. N., Aryal, D., Osti, N. C., He, L. L., Heller, W. T., Willis, C. L., … Perahia, D. (2016) Association of a multifunctional ionic block copolymer in a selective solvent. *Journal of Chemical Physics*, **145**:9.

Foster, B., Cosgrove, T., & Hammouda, B. (2009) Pluronic Triblock copolymer systems and their interactions with ibuprofen. *Langmuir*, **25**:6760–6766.

Ghaouar, N., Baroudi, M., & Othman, T. (2016) Contribution to the explanation of the association process of two triblock poly(ethylene oxide)-poly(propylene oxide)-poly(ethylene oxide) (PEO-PPO-PEO) copolymers and their mixtures in an aqueous solution. *Journal of Molecular Liquids*, **224**:279–283.

Guo, C., Liu, V., & Chen, J. Y. (2000) A Fourier transform infrared study on water-induced reverse micelle formation of block copoly(oxyethylene-oxypropylene-oxyethylene) in organic solvent. *Colloids and Surfaces A-Physicochemical and Engineering Aspects*, **175**:193–202.

Herfurth, C., Laschewsky, V., Noirez, L., von Lospichl, B., & Gradzielski, M. (2016) Thermoresponsive (star) block copolymers from one-pot sequential RAFT polymerizations and their self-assembly in aqueous solution. *Polymer*, **107**:422–433.

Hinze, W. L., & Pramauro, E. (1993) A critical-review of surfactant-mediated phase separations (cloud-point extractions) – Theory and applications. *Critical Reviews in Analytical Chemistry*, **24**: 133–177.

Holmberg, K., Jonsson, B., Kronberg, B., & Lindman, B. (2002) *Surfactants and polymers in aqueous solution* (2nd ed.). West Sussex: John Wiley & Sons.

Israelachvili, J. N., Mitchell, D. J., & Ninham, B. W. (1976) Theory of self-assembly of hydrocarbon amphiphiles into micelles and bilayers. *Journal of the Chemical Society-Faraday Transactions Ii*, **72**: 1525–1568.

Ivanova, R., Lindman, B., & Alexandridis, P. (2000) Effect of glycols on the self-assembly of amphiphilic block copolymers in water. 1. Phase diagrams and structure identification. *Langmuir*, **16**: 3660–3675.

Jia, L. W., Guo, C., Yang, L. R., Xiang, J. F., Tang, J. F., Liu, C. Z., & Liu, H. Z. (2010) Mechanism of PEO-PPO-PEO micellization in aqueous solutions studied by two-dimensional correlation FTIR spectroscopy. *Journal of Colloid and Interface Science*, **345**:332–337.

Kadam, Y., Singh, K., Marangoni, D. G., Ma, J. H., Aswal, V. K., & Bahadur, P. (2010) Thermodynamic of micelle formation of nonlinear block co-polymer Tetronic (R) T904 in aqueous salt solution. *Colloids and Surfaces A-Physicochemical and Engineering Aspects*, **369**:121–127.

Karlstrom, G. (1985) A new model for upper and lower critical solution temperatures in poly(ethylene oxide) solutions. *Journal of Physical Chemistry*, **89**:4962–4964.

Kinning, D. J., & Thomas, E. L. (1984) Hard-sphere interactions between spherical domains in diblock copolymers. *Macromolecules*, **17**:1712–1718.

Kjellander, R. (1982) Phase-separation of non-ionic surfactant solutions – A treatment of the micellar interaction and form. *Journal of the Chemical Society-Faraday Transactions Ii*, **78**:2025–2042.

Kjellander, R., & Florin, E. (1981) Water-structure and changes in thermal-stability of the system poly(ethylene oxide)-water. *Journal of the Chemical Society-Faraday Transactions I*, **77**:2053–2077.

Kotlarchyk, M., & Chen, S. H. (1983) Analysis of small-angle neutron-scattering spectra from polydisperse interacting colloids. *Journal of Chemical Physics*, **79**:2461–2469.

Kwon, G. S., & Okano, T. (1996) Polymeric micelles as new drug carriers. *Advanced Drug Delivery Reviews*, **21**:107–116.

Lee, J. H., Lee, H. B., & Andrade, J. D. (1995) Blood compatibility of polyethylene oxide surfaces. *Progress in Polymer Science*, **20**: 1043–1079.

Lindman, B., & Karlstrom, G. (2009) Nonionic polymers and surfactants: Temperature anomalies revisited. *Comptes Rendus Chimie*, **12**:121–128.

Liu, T. B., Nace, V. M., & Chu, B. (1997a) Cloud-point temperatures of BnEmBn and PnEmPn type triblock copolymers in aqueous solution. *Journal of Physical Chemistry B*, **101**:8074–8078.

Liu, T. B., Zhou, Z. K., Wu, C. H., Nace, V. M., & Chu, B. (1997b) Effects of block lengths on the association numbers and micellar sizes of BnEmBn type triblock copolymer micelles in aqueous solution. *Macromolecules*, **30**:7624–7626.

Lobry, L., Micali, N., Mallamace, F., Liao, C., & Chen, S. H. (1999) Interaction and percolation in the L64 triblock copolymer micellar system. *Physical Review E*, **60**:7076–7087.

Malmsten, M., & Lindman, B. (1992) Self-assembly in aqueous block copolymer solutions. *Macromolecules*, **25**:5440–5445.

Misra, S. K., & Skold, R. O. (2000) Lubrication studies of aqueous mixtures of inversely soluble components. *Colloids and Surfaces A: Physicochemical and Engineering Aspects*, **170**:91–106.

Misra, S. K., & Skold, R. O. (2001) Phase and aggregational studies of some inversely soluble aqueous formulations. *Colloids and Surfaces A: Physicochemical and Engineering Aspects*, **179**:114–124.

Miyazaki, S., Ohkawa, Y., Takada, M., & Attwood, D. (1992) Antitumor effect of pluronic F-127 gel containing mitomycin-C on sarcoma-180 ascites. *Chemical & Pharmaceutical Bulletin*, **40**: 2224–2226.

Miyazaki, S., Tobiyama, T., Takada, M., & Attwood, D. (1995) Percutaneous-absorption of indomethacin from pluronic F127 gels in rats. *Journal of Pharmacy and Pharmacology*, **47**:455–457.

Mortensen, K. (1992) Phase-behavior of poly(ethylene oxide)-poly (propylene oxide)-poly(ethylene oxide) triblock-copolymer dissolved in water. *Europhysics Letters*, **19**:599–604.

Mortensen, K., & Pedersen, J. S. (1993) Structural study on the micelle formation of poly(ethylene oxide) poly(propylene oxide) poly(ethylene oxide) triblock copolymer in aqueous-solution. *Macromolecules*, **26**:805–812.

Németh, Z., Rácz, G., & Koczo, K. (1998) Foam control by silicone polyethers—Mechanisms of "cloud point antifoaming". *Journal of Colloid and Interface Science*, **207**:386–394.

Nishikawa, K., Kodera, Y., & Iijima, T. (1987) Fluctuations in the particle number and concentration and the Kirkwood-Buff parameters of tert-butyl alcohol and water mixtures studied by small-angle x-ray scattering. *Journal of Physical Chemistry*, **91**:3694–3699.

Pandit, N. K., & Mclntyre, H. (1997) Cosolvent effects on the gel formation and gel melting transitions of pluronic F127 gels. *Pharmaceutical Development and Technology*, **2**:181–184.

Parekh, P., Singh, K., Marangoni, D. G., & Bahadur, P. (2012) Effect of alcohols on aqueous micellar solutions of PEO-PPO-PEO copolymers: A dynamic light scattering and H-1 NMR study. *Journal of Molecular Liquids*, **165**:49–54.

Park, M. J., & Char, K. (2004) Gelation of PEO-PLGA-PEO triblock copolymers induced by macroscopic phase separation. *Langmuir*, **20**:2456–2465.

Patel, K., Bharatiya, B., Kadam, Y., & Bahadur, P. (2010) Micellization and clouding behavior of EO-PO block copolymer in aqueous salt solutions. *Journal of Surfactants and Detergents*, **13**: 89–95.

Patel, T., Bahadur, P., & Mata, J. (2010) The clouding behaviour of PEO-PPO based triblock copolymers in aqueous ionic surfactant solutions: A new approach for cloud point measurements. *Journal of Colloid and Interface Science*, **345**:346–350.

Pedersen, J. S. (1997) Analysis of small-angle scattering data from colloids and polymer solutions: Modeling and least-squares fitting. *Advances in Colloid and Interface Science*, **70**:171–210.

Pelton, R. (2002) A review of antifoam mechanisms in fermentation. *Journal of Industrial Microbiology & Biotechnology*, **29**:149–154.

Pillai, S. A., Sheth, U., Bahadur, A., Aswal, V. K., & Bahadur, P. (2016) Salt induced micellar growth in aqueous solutions of a star block copolymer Tetronic (R) 1304: Investigating the role in

solubilizing, release and cytotoxicity of model drugs. *Journal of Molecular Liquids*, **224**:303–310.

Pitard, B., Pollard, H., Agbulut, O., Lambert, O., Vilquin, J. T., Cherel, Y., … Escande, D. (2002) A nonionic amphiphile agent promotes gene delivery in vivo to skeletal and cardiac muscles. *Human Gene Therapy*, **13**:1767–1775.

Reddy, N. K., Fordham, P. J., Attwood, D., & Booth, C. (1990) Association and surface-properties of block-copoly-(oxyethylene oxypropylene oxyethylene) L64. *Journal of the Chemical Society-Faraday Transactions*, **86**:1569–1572.

Schönfeldt, N. (1969) *Surface active ethylene oxide adducts*. London: Pergamon Press.

Sharma, P. K., Reilly, M. J., Bhatia, S. K., Sakhitab, N., Archambault, J. D., & Bhatia, S. R. (2008a) Effect of pharmaceuticals on thermoreversible gelation of PEO-PPO-PEO copolymers. *Colloids and Surfaces B-Biointerfaces*, **63**:229–235.

Sharma, P. K., Reilly, M. J., Jones, D. N., Robinson, P. M., & Bhatia, S. R. (2008b) The effect of pharmaceuticals on the nanoscale structure of PEO-PPO-PEO micelles. *Colloids and Surfaces B-Biointerfaces*, **61**:53–60.

Shen, Y., & Wu, P. Y. (2003) Two-dimensional ATR-FTIR spectroscopic investigation on water diffusion in polypropylene film: Water bending vibration. *Journal of Physical Chemistry B*, **107**: 4224–4226.

Su, Y. L., Wang, J., & Liu, H. Z. (2002a) FTIR spectroscopic investigation of effects of temperature and concentration on PEO-PPO-PEO block copolymer properties in aqueous solutions. *Macromolecules*, **35**:6426–6431.

Su, Y. L., Wang, J., & Liu, H. Z. (2002b) FTIR spectroscopic study on effects of temperature and polymer composition on the structural properties of PEO-PPO-PEO block copolymer micelles. *Langmuir*, **18**:5370–5374.

Svensson, B., Alexandridis, P., & Olsson, U. (1998) Self-assembly of a poly(ethylene oxide) poly(propylene oxide) block copolymer (Pluronic P104, (EO)(27)(PO)(61)(EO)(27)) in the presence of water and xylene. *Journal of Physical Chemistry B*, **102**: 7541–7548.

Svensson, M., Alexandridis, P., & Linse, P. (1999) Phase behavior and microstructure in binary block copolymer/selective solvent systems: Experiments and theory. *Macromolecules*, **32**:637–645.

Teixeira, C. V., Amenitsch, H., Fukushima, T., Hill, J. P., Jin, W., Aida, T., … Linden, M. (2010) Form factor of an N-layered helical tape and its application to nanotube formation of hexa-perihexabenzocoronene-based molecules. *Journal of Applied Crystallography*, **43**:850–857.

Teixeira, C. V., Amenitsch, H., Linton, P., Linden, M., & Alfredsson, V. (2011) The role played by salts in the formation of SBA-15, an in situ small-angle X-ray scattering/diffraction study. *Langmuir*, **27**:7121–7131.

Tew, G. N., Sanabria-DeLong, N., Agrawal, S. K., & Bhatia, S. R. (2005) New properties from PLA-PEO-PLA hydrogels. *Soft Matter*, **1**:253–258.

Viti, V., & Zampetti, P. (1973) Dielectric properties of 2-methoxyethanol and 1,2-dimethoxyethane: Comparison with ethylene glycol. *Chemical Physics*, **2**:233–238.

Wang, Z. L., & Feng, H. (2010) Double cloud point of ethylene oxide-propylene oxide triblock copolymer in an aqueous solution. *Colloids and Surfaces a-Physicochemical and Engineering Aspects*, **362**:110–116.

Wanka, G., Hoffmann, H., & Ulbricht, W. (1990) The aggregation behavior of poly-(oxyethylene)-poly-(oxypropylene)-poly-(oxyethylene)-block-copolymer in aqueous-solution. *Colloid and Polymer Science*, **268**:101–117.

Wanka, G., Hoffmann, H., & Ulbricht, W. (1994) Phase-diagrams and aggregation behavior of poly(oxyethylene)-poly(oxypropylene)-poly(oxyethylene) triblock copolymers in aqueous-solutions. *Macromolecules*, **27**:4145–4159.

Watanabe, H., & Tanaka, H. (1978) Nonionic surfactant as a new solvent for liquid-liquid – Extraction of zinc(II) with 1-(2-pyridylazo)-2-naphtol. *Talanta*, **25**:585–589.

Zhang, H., Yu, L., & Ding, J. D. (2008a) Roles of hydrophilic homopolymers on the hydrophobic-association-induced physical gelling of amphiphilic block copolymers in water. *Macromolecules*, **41**: 6493–6499.

Zhang, J., Gassmann, M., Chen, X. M., Burger, X. M., Rong, L. X., Ying, Q. C., & Chu, B. (2007) Characterization of a reversible thermoresponsive gel and its application to oligonucleotide separation. *Macromolecules*, **40**:5537–5544.

Zhang, J. B., Zhang, P. Y., Ma, K., Han, F., Chen, G. H., & Wei, X. H. (2008b) Hydrogen bonding interactions between ethylene glycol and water: Density, excess molar volume, and spectral study. *Science in China Series B-Chemistry*, **51**:420–426.

Zhou, Z., & Chu, B. (1994) Phase-behavior and association properties of poly(oxypropylene)-poly(oxythylene)-poly(oxypropylene) triblock copolymer in aqueous-solution. *Macromolecules*, **27**: 2025–2033.

Zhou, Z. K., & Chu, B. (1988a) Anomalous micellization behavior and composition heterogeneity of a triblock ABA copolymer of (A) ethylene-oxide and (B) propylene-oxide in aqueous-solution. *Macromolecules*, **21**:2548–2554.

Zhou, Z. K., & Chu, B. (1988b) Light-scattering study on the association behavior of triblock polymers of ethylene-oxide and propylene-oxide in aqueous-solution. *Journal of Colloid and Interface Science*, **126**:171–180.